

Development of a Smart Wearable Device for Fall and Slip Detection and Warning for the Elderly People

Thanh Huong Nguyen, Viet Tung Nguyen*

School of Electrical and Electronic Engineering, Hanoi University of Science and Technology, Ha Noi, Vietnam

*Corresponding author email: tung.nguyenviet@hust.edu.vn

Abstract

In the elderly, due to the degeneration of the muscles along with visual impairment, mobility becomes more difficult than in other ages. Upon moving, the elderly can be susceptible to several factors such as slips or obstacles which can cause unintended fall events and can lead to different degrees of injury, from minor trauma to more severe and even life-threatening injuries. In this work, the characteristics of movement and falling in the elderly are first studied, thereby finding thresholds for determining fall events for motion parameters to detect ahead of time the fall event. Therefore, necessary warnings can be promptly delivered to the users or caregivers, otherwise distress signal can be sent wirelessly to request assistance if the elderly is unable to stand up. This will help minimize the negative impact on the elderly caused by the fall event. The paper proposes to base the research on motion and fall features of the old people to build a wearable device which combines gyroscope accelerometer, a self-developed fall sensor and heart rate sensor for fall detection and warning. The device also employs parameter thresholds to detect forward and backward fall events as well as to provide accurate information about other familiar activities such as standing and sitting, lean forward, backward, left or right. The threshold-based method we used in determining the body states correctly identified the states: 93.33% steady state, 86.67% fallible state and 96.67% slip state. Moreover, the device can also achieve 90% accurate information about the user's heart rate.

Keywords: Elderly, fall, slip, detection, warning, sensor, wearable device.

1. Introduction

Anyone over the age of sixties can experience health and physical risks. Common risks are slip and fall that occur due to minor injuries, loss of balance, heart problems, drug side effects, external environmental influences and so on. According to the American Society of Geriatrics, one quarter of population over the age of 65 have slipped and fallen more than once [1]. Elderly people who have weak immune systems also suffer from underlying medical conditions that lead to injuries from falls. In addition, they hardly recover compared to other people or cannot fully recover. In Vietnam, every year, 1.5 or 1.9 million people slipped and fell and 5% of them come down with injuries that require special health care [2]. Depending on the severity of the fall, injuries can affect motor function or even lead to death. At the Department of Geriatrics - Palliative Care, Ho Chi Minh City University of Medicine and Pharmacy, every month, about 17% of patients are hospitalized due to falls or fall-related events [3]. Elderly patients who suffer from impaired moving organism also cope with mobility struggle in daily living, even the need the care and monitoring from family member or medical staff. In addition to negative effects on physical health, falls also affect the mental health of

the person who fell. A fear of falling will appear, making the elderly become afraid and inactive. This creates a heavy burden to the family and society. It is for such reasons that a device that can detect and warn the elderly is necessary to be constructed for wearing on human body every day.

There are several methods that have been used to detect falls for the elderly: threshold detection, non-threshold and fusion-based detection [4, 5] as illustrated in Fig. 1 which is simplified drawn from article of Kadhum *et al.*

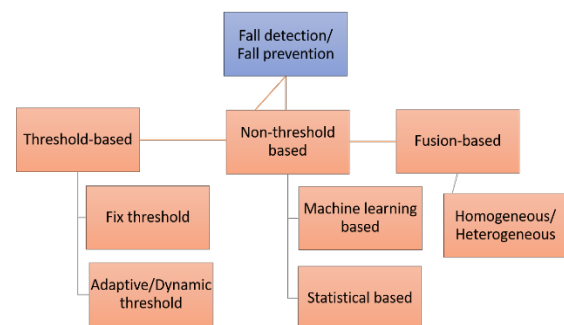


Fig. 1. Fall detection/ fall prevention method classification

Threshold-based method makes use of motion sensors such as accelerometer [6], gyroscope [7], magnetometer [8], inertial sensors [9] or combining some of them to detect the body states, perceive the sign of falling and activate the alarm. In this method, appropriate threshold value must be chosen if using specific sensor and dynamic values if multiple sensors are involved [10-12]. The reason for the selection is because low threshold may lead to false warning while high threshold can cause missing falls [13]. Those above-mentioned methods are applied to fall detection mainly based on the threshold or non-threshold approaches. The non-threshold-based method utilizes principally machine learning in which the images obtained from the camera, the vibration or sound on the floor are processed to identify the falls and slip. These methods have high accuracy but have high cost, large size, substantial power consumption and only favorable for static devices.

Recent health monitoring systems have focused on detecting and reporting various falls and slips in real time. These research efforts yield relatively high accuracy. However, previously proposed solutions were limited to specific falls and slips, were too complex or expensive. Some methods are only used to identify, interpret, and monitor various activities of daily living and report falls. There is research number [11] on wearable sensors and embedded microelectromechanical systems (MEMS), which provide vital signs such as movement, heart and respiratory status. To detect falls, sensors are used to evaluate different body posture and movement patterns as the patient engages in different activities. Linked to a microcontroller and/or mobile phone, the motion tracker provides information about angular acceleration, body orientation, and magnetic field changes caused by motion caused in different directions. The data obtained can then be processed using machine learning algorithms to give an accurate picture of different types of activities. However, this system has environmental or privacy concerns and their performance.

In [14], the research team developed an online smartphone system to detect falls with warning notifications. This system uses accelerometers and gyroscopes of sensors embedded in smartphones to track participants' movement patterns. Using a federated cloud-based regression model, the system succeeded in detecting 27 of the 37 falls that occurred with a sensitivity of 73.0% and resulted in one false alarm every time after 46 days over a period of 2070 days and 23 individuals participated. It can be seen that the sensitivity of the above system is not high.

Another system in [15] develops a wearable motion tracker with accelerometer and gyroscope sensors to generate data about a person's movement patterns. Based on UMA activity dataset collected

from 19 subjects at Universidad de Málaga, wearable trackers placed in five different locations on the body were obtained. Then, a recurrent neural network (RNN)-based model is developed to analyze a series of time intervals and detect falls from other daily life activities. The system produced results with 92.31% accuracy, yielding a relatively accurate indication of fall events, but this study was performed on a sample data set and there was no real-world testing.

Another research group detected falls using ambient sensors. Some applications of external sensors are pre-installed for motion tracking, which does not require the user to wear specialized equipment, providing a seamless solution without any difficulty even if the user forgets to wear the device. A good example is a piezoelectric vibration detector on the floor to detect falls because everyday activities cause detectable vibrations on the floor in patterns other than those of falls. When falling to the floor, the vibrations created will have some distinct characteristics, then the [16] research team used the K-means and K nearest neighbor algorithms to classify with 91% accuracy in detecting human falls from different positions. Sound sensors and pressure sensors are two basic types of sensors for detecting vibrations. Although this method provides high accuracy at a low cost, the type of floor has a large influence on the detection range of the vibration sensor, thus leading to unpleasant deviations in the results. Another insurmountable drawback of ambient vibration classification is that the excessive amount of noise generated by background noise reduces accuracy, leading to many false positive predictions.

The recent methods of determining by different kinds of sensor to track motion have relatively high accuracy, but the processing approach requires complicated processing methods which requires high price computation platform and not applicable to multiple cases. On the contrary, threshold detection has lower accuracy, but in return this method has the advantages of compact equipment, low energy consumption, moderate cost and suitable for devices worn on the body. For the purpose of making an on-body wearable device, in this study, we propose a device for detecting and warning falls for the elderly which allows to warn the elderly about cases of unsteady steps that can slip and fall. Besides, it can provide important information about the state of the body of the elderly to medical staff or relative caregivers so that they can promptly provide necessary support in case of slip and fall, thus helping them to avoid serious injury. In addition, the device needs to have heart rate monitoring capability from which it can monitor the patient's health. In order to gather the threshold information for the device, several components are integrated into the whole system: (1) 3D accelerometer sensor - a six-degree-of-freedom gyroscope, (2) self-designed optical sensor device,

(3) electrocardiogram sensor, (4) microcontroller and (5) connection device. The accelerometer and optical sensor are in charge of collecting information about body movements, then transmit to the microcontroller to determine the state of the body. Thanks to the data acquisition from the sensors, the system is able to detect the body states of the elderly people such as falling forward, falling backward, standing, sitting, tilting to the left, tilting to the right and slipping. The device also possesses a built-in heart rate sensor that performs a heart rate measurement which permits the patient to check their own heart rate if needed.

The device prototype was placed and attached on real human body and its performance was validated by determining body states. Based on the threshold-based method, the obtained device can detect several states with the accuracy of 93.33% steady state, 86.67% fallible state and 96.67% slip state and 90% accurate information about the user's heart rate.

2. Theoretical Principle of Proposed Components

In this study, in order to build a wearable wireless system, the chosen method used here is the method to determine the slip and fall based on the limiting thresholds of the motion parameters of the human body. To be able to consider the threshold, the parameters of the motion are selected: acceleration of the three sensor axes, aggregate acceleration, and orientation angles (pitch and roll angles). In this section, the sensors and their parameters are described in detail.

2.1. 3D Accelerometer - Six-Degree-of-Freedom Gyroscope

The accelerometer has low accuracy because the accelerometer's weight is very small resulting in it being heavily influenced by external forces even when the external forces are very small. In contrast, the gyroscope is highly accurate. The selected sensor for this system is the MPU-6050 sensor [14] as shown in Fig. 2. This sensor not only allows to access the acceleration of the three axes but also permits determining the angular acceleration around the three axes mentioned above. Sensitivity for accelerometer can be up to 16g while the sensitivity for gyroscope can be up to 2000°/s. This sensor favors communication with the microcontroller through the I²C protocol.

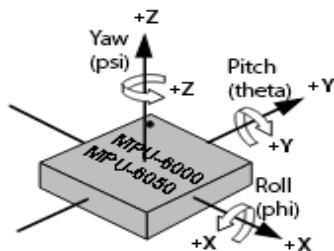


Fig. 2. Gyroscope (Six-degree-of-freedom accelerometer)

This MEM accelerometer is designed to measure static and dynamic accelerations based on the acceleration acting directly on the three-sensor axis x , y and z . Static acceleration is the acceleration produced by a constant force acting on the sensor while dynamic acceleration is the acceleration that changes as the sensor movement. At the same time, the device also provokes the angular speed of the axes. The acceleration acting on each sensor axis is an inertial acceleration and is expressed in units of “g” with 1g is 9,806 m/s². The data obtained from the gyroscope is the variable speed of the pitch, roll, and yaw angles and is expressed in units of: °/s.

a) Three-axis acceleration

The sensor is used to determine the orientation of the body during movement by using the data obtained from the sensor to calculate the total acceleration and orientation angles.

If the total acceleration of motion is A , the data from the 3D accelerometer sensor is the acceleration acting on the weight on the three axes a_x , a_y and a_z (as shown in Fig. 3). These values are also the projected values of A on the three axes of the sensor.

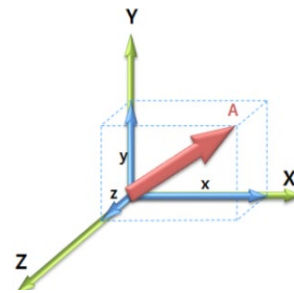


Fig. 3. Gyroscope (Six-degree-of-freedom accelerometer)

This total acceleration A is calculated as follows:

$$\vec{A} = \vec{a}_x + \vec{a}_y + \vec{a}_z \quad (1)$$

and
$$A = \sqrt{a_x^2 + a_y^2 + a_z^2} \quad (2)$$

b) Orientation angles

Every movement of the object can be attributed to the variation of orientation angles. They are three spacious angles: pitch, roll and yaw (Fig. 4).

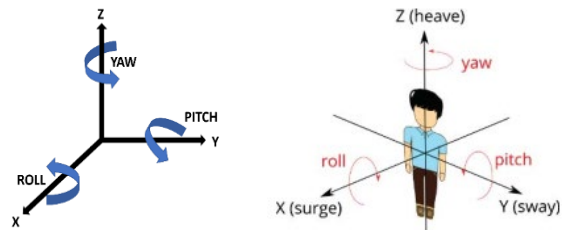


Fig. 4. Directional angles (pitch, roll, yaw): Left - On the 3D axis; Right - On the designed object.

In this study, we only consider fall events and some common activities of the elderly, so the yaw angle is not considered because the movement rotating in place is not considered. From the obtained raw data, pitch and roll orientation angles can be calculated in the following equations.

Pitch and roll orientation angles are calculated from accelerometer data as follows:

$$\text{Pitch: } \theta_{acc} = \arctan\left(\frac{a_x}{\sqrt{a_y^2 + a_z^2}}\right) \quad (3)$$

$$\text{Roll: } \rho_{acc} = \arctan\left(\frac{a_y}{\sqrt{a_x^2 + a_z^2}}\right) \quad (4)$$

Pitch and roll orientation angles are calculated from the gyroscope data as follows:

$$\text{Pitch: } \theta_{gyro} = \theta_{gyro,0} + \int_{t_0}^t g_y dt \quad (5)$$

$$\text{Roll: } \rho_{gyro} = \rho_{gyro,0} + \int_{t_0}^t g_x dt \quad (6)$$

Owing to the 3D accelerometer, we get the data on the rate of change of the roll and pitch angles over time, respectively: g_x and g_y . Assuming from the time t_0 to t , the initial values of pitch and roll are varying from $\theta_{gyro,0}$, $\rho_{gyro,0}$, the total values of pitch and roll angles α and β are used as parameters to decide the states of object. These total values are calculated as follows:

$$\text{Total pitch: } \alpha = k_{acc} \cdot \theta_{acc} + k_{gyro} \cdot \theta_{gyro} \quad (7)$$

$$\text{Total roll: } \beta = k_{acc} \cdot \rho_{acc} + k_{gyro} \cdot \rho_{gyro} \quad (8)$$

where k_{acc} and k_{gyro} are the weights of priority to express the relationship between the accuracy of the accelerometer and gyroscope. Normally, the gyroscope retains high accuracy and is less affected by external forces while the accelerometer is on the contrary. Hence, the above-mentioned two weights should be chosen $k_{acc} = 0.1$ and $k_{gyro} = 0.9$.

2.2. Self-Designed Optical Sensor

For better recognition of slip and fall, in addition to accelerometer, in this study, a state detection sensor based on optical signal is proposed as shown in Fig. 5.

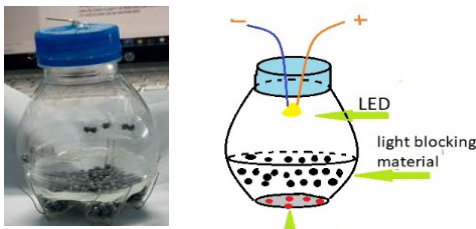


Fig. 5. Self-designed optical sensor

The device consists of a hollow cavity containing iron balls (in Fig. 6b) that block light, covering about a third of the cavity from the bottom. The top of the compartment is arranged with a red LED (Light Emitting Diode) that is always turned on and five photo resistive sensors (in Fig. 6a) placed at the bottom of the cavity at equal angles.

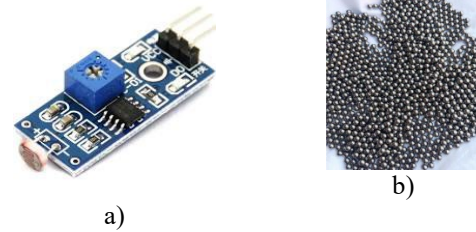


Fig. 6. a) Photo resistive sensor; b) Iron balls used as light blocking material

The idea for this device is based on the relatively slow daily actions of the elderly. For daily activities performed slowly by the elderly, the external force applied to the device is not enough to be able to move the iron ball layers leading to the optical sensors that can detect light. But when a fall event occurs, the external force acting on the device is large enough then the iron ball layers will be displaced and exposed to the optical sensors from which they can sense the light emitted from LED. The principle of this self-designed sensor is to create logic output of 0 or 1 to detect the sudden change of the body. As a result, when the fall event has been determined by the motion parameter thresholds, the optical sensor can sense the light even though a real fall event quickly emerges without any additional complicated calculations. This proposed component is designed to use five optical sensors to increase the sensitivity of the device.

2.3. Heart Rate Sensor

Heart rate is characterized by the number of contractions of the heart per minute or the number of heart cycles per minute. Heart rate in each person, each age is different. Heart rate is only considered when the body is in a state of rest and does not have to perform vigorous activities. In one minute, the number of heart cycles obtained can be computed as:

$$BPM = \frac{60}{T} \text{ (beats/min)} \quad (9)$$

Table 1. Heart rate at each age

Age	Heart rate standard (beats/min)
Infant	120 - 160
1 to 12-month-old child	80 - 140
1 to 2-year-old child	80 - 130
2 to 6-year-old child	75 - 120
7 to 12-year-old child	75 - 110
Adult	60 - 100
Athletes	40 - 60

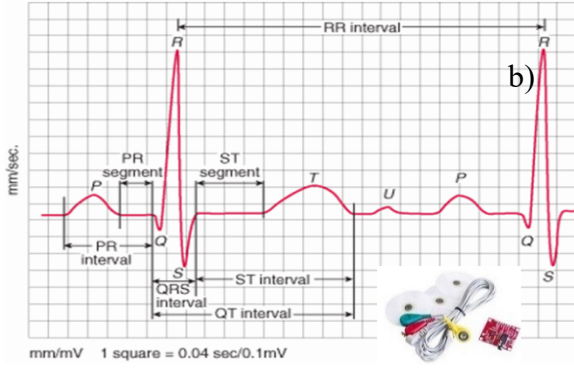


Fig. 7. a) ECG diagram; b) AD8232 sensor

For measuring this heart rate with high accuracy, the electrocardiogram (ECG) method is employed. ECG is a method of monitoring the activity, speed, and rhythm of the heart. When the heart is working, it contracts and emits variations of the electric current, a curve that records those variations is derived as ECG. Through reading the ECG, we can know the heart's ability to eject blood, the rhythm and speed of the heart. The sensor AD8232 of Analog Device (Fig. 7b) enables reading electrical signals of the heart then generates ECG graphs (Fig.7a) to survey the activity of the heart as well as determine the heart rate.

The human heart is made up of four chambers to carry out the function of storing and pumping blood throughout the body, two small atria and two larger ventricles. Blood flows from the veins to the right atrium and from the lungs to the left atrium. Squeezing the left atrium pumps blood into the left ventricle, and the right atrium pumps blood into the right ventricle. The right ventricle then squeezes to pump blood through the arteries to the lungs, and the left ventricle squeezes to pump blood down the body. The sinuses in the right atrium are made up of cells capable of emitting electrical impulses. These electrical impulses propagate to the surrounding cells, causing the two atria to contract (forming *P* waves). After that, the current continues to pass along a special cell chain to the atrioventricular node located near the interventricular septum, and then along the Purkinje fiber cell chain running along the interventricular septum and spreading into the surrounding the two ventricle muscles (generating a series of *QRS* waves). Then, the electrical impulses decrease, the ventricles relax (creating a *T* wave). From Fig. 7a, the time interval between two consecutive *R* peaks of the ECG signal is the *T* cycle of the heart.

3. Algorithms for Threshold-Based Fall and Slip Detection

The fall and slip can cause severe consequences to the elderly and cannot be detected solely owing to the accelerometer data. In Section 2, we mentioned another two sensors as the data acquisition component for the computer to process. However, to combine all

three types of sensors, it is important to implement the suitable algorithm to reach the accurate orientation information. Thanks to the threshold-based classification method [10-12], we proposed the appropriate algorithms to assess the body state as well as evaluate the heart rate data.

3.1. Body State Detection Algorithm

When using the device, we are only interested in identifying and warning of falls or can recognize the earliest slip and fall. Therefore, four states are involved:

- S_0 (stable state) is the state of the body when standing or sitting.
- S_1 (slippable state) is the state that includes the actions of leaning forward, backward, left or right.
- S_2 (testing state) is the slip state that has been determined by the accelerometer sensor but has not been checked by the optical sensor.
- S_3 (slipped down state) is the completely confirmed slip state.

Based on the divided four states, an algorithm is derived in Fig. 8. The data obtained from accelerometer and optical sensor are used to determine different S_i states of the body.

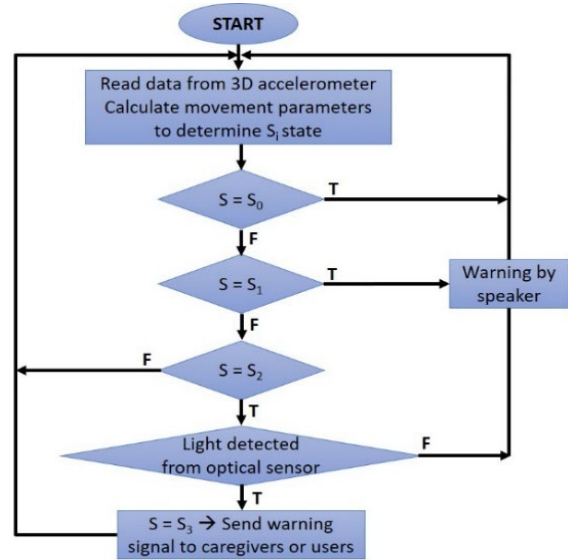


Fig. 8. Algorithm to detect different body states

3.2. Heart Rate Determination Algorithm

The idea of the algorithm is to determine the time interval between two occurrences of the peak *R* of the consecutive *ECG* signal. This interval is called the sample (millisecond). Thus, we can calculate the number of heartbeats in one minute as follows:

$$BPM = 60 \cdot \frac{1000}{sample} \quad (beats/min) \quad (10)$$

The determination of R points and the time interval between two consecutive R points is done as the following flowchart in Fig. 9.

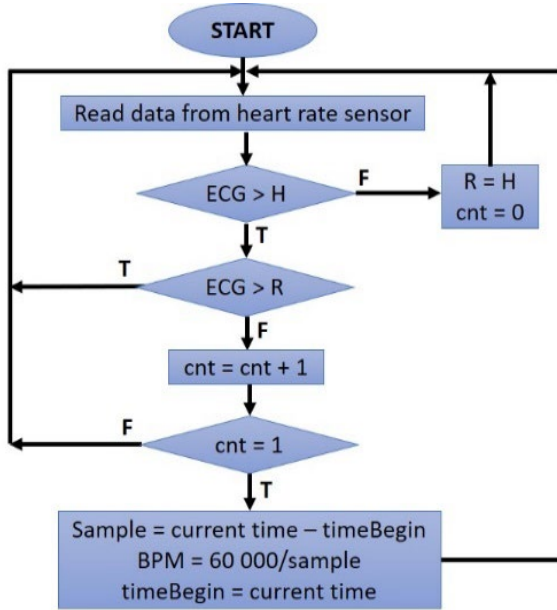


Fig. 9. Algorithm to determine heart rate

According to Fig. 9, the heart rate determining algorithm has some specific notation.

- To avoid misjudging the point T or P into the point R , we need a certain threshold to start the vertex finding algorithm.

- The threshold as the value of the peak T needs to be chosen according to the conditions:

+ When the measured value of $ECG > H$, we start to find the peak R as follows (R is initially set to H): If $ECG > R \rightarrow R = ECG$; If $ECG < R$ (i.e. ECG has reached the RS flank): $cnt = cnt + 1$; when $cnt = 1$ means the ECG is at the first point of the RS flank.

+ The jump between the times of taking the signal from the sensor is very small, so this point can be considered as the R point, this time is taken to start calculating the sample value ($timeBegin$):

$$\text{Sample} = \text{current time value} - \text{timeBegin.}$$

- When the ECG measurement value is smaller than H then clear cnt and reset R with H in preparation for the next R search. From such initial analysis, we have the algorithm flowchart for the heart rate sensor block as in Fig. 9.

4. Experimental Results

Based on the design ideas mentioned above, the product after designing is displayed in Fig. 10.



Fig. 10. Wearable device prototype

In this section, we will present the process of determining the thresholds of the parameters and the results of the identification of states. We are interested in three following states:

- Steady state: Includes the act of standing upright and sitting upright.
- Falling risky state: Includes actions of leaning forward, backward, leaning to the right, and the left.
- Slipped state: Includes forward and backward falls

4.1. Single Action Test Result

The state experiments for fall and slip detection are illustrated in Fig. 11. In the experimental setup, the testing person wear it on the belly because that place responds the fastest and clearest of the falling and slipping. The experimental scenarios is conducted based on states: steady state, slipped state and fallible states. The steady state accounts for sitting or standing upright. The fallible state includes four cases such as leaning forward, backward, leaning to the right, and to the left. The slipped state contained forward and backward fall. For each state, we measured the set of limiting thresholds and calculated the average values which are mentioned in Table 2.



Fig. 11. Illustration for different states

To assess the accuracy of the experiments, we derive an equation in which the accuracy is the number of the correct recognition (indicated by T - true in Table 3) among total number of test. The formulation is as followed:

$$\gamma = \frac{N_T}{N_{total}} \times 100\% \quad (11)$$

where: γ is the accuracy in percentage, N_T is the number of correct detection (Table 3 - case of T) and N_{total} is the total number of test.

The experiment for each posture was carried out 10 times, we obtained the threshold values for acceleration and orientation in Fig. 12 and Fig. 13.

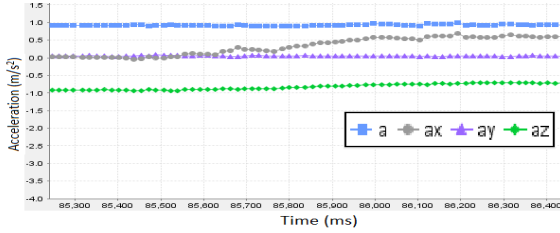


Fig. 12. Acceleration of different axes and total acceleration when changing from standing upright to leaning forward

The experiment was conducted similarly for other actions and states, we obtained the limiting thresholds of all parameters for each single activity shown in Table 2 and Table 3.

Table 2. The limiting thresholds of the parameters for the single action

<i>Parameter</i>	<i>Falling forward</i>	<i>Falling backward</i>	<i>Standing /Sitting</i>	<i>Tilting forward</i>	<i>Tilting backward</i>	<i>Tilting to the left</i>	<i>Tilting to the right</i>
a_x	(1; 1.25)	(-1.25; -1)	(-0.3; 0.3)	(0.3; 0.5)	(-0.5; -0.3)	(-0.3; 0.3)	(-0.3; 0.3)
a_y	(-0.1; 0.1)	(-0.1; 0.1)	(-0.3; 0.3)	(-0.3; 0.3)	(-0.3; 0.3)	(0.3; 0.5)	(-0.5; -0.3)
a_z	(-0.1; 0.1)	(-0.1; 0.1)	(-1; -0.8)	(-0.8; -0.75)	(-0.8; -0.75)	(-0.8; -0.75)	(-0.8; -0.75)
A	(1.25; 2)	(1.25; 2)	(0.9; 1)	(0.9; 1)	(0.9; 1)	(0.9; 1)	(0.9; 1)
α	(60; 90)	(-90; -60)	(-15; 15)	(20; 35)	(-35; -20)	(-15; 15)	(-15; 15)
β	(-15; 15)	(-15; 15)	(-15; 15)	(-15; 15)	(-15; 15)	(20; 35)	(-35; -20)

Table 3. Body state recognition results (T = True; F = False)

Testing time	1	2	3	4	5	6	7	8	9	10	11	12	13	14	15
<i>Stable state</i>	T	T	T	T	T	T	T	T	T	T	T	F	T	T	T
<i>Fallible state</i>	T	T	T	T	F	T	T	T	T	T	T	T	T	F	T
<i>Slipped down state</i>	T	T	T	T	T	T	T	T	T	T	T	F	T	T	T
Testing time	16	17	18	19	20	21	22	23	24	25	26	27	28	29	30
<i>Stable state</i>	T	T	T	T	T	T	T	F	T	T	T	T	T	T	T
<i>Fallible state</i>	T	T	F	T	T	T	T	T	F	T	T	T	T	T	T
<i>Slipped down state</i>	T	T	T	T	T	T	T	T	T	T	T	T	T	T	T

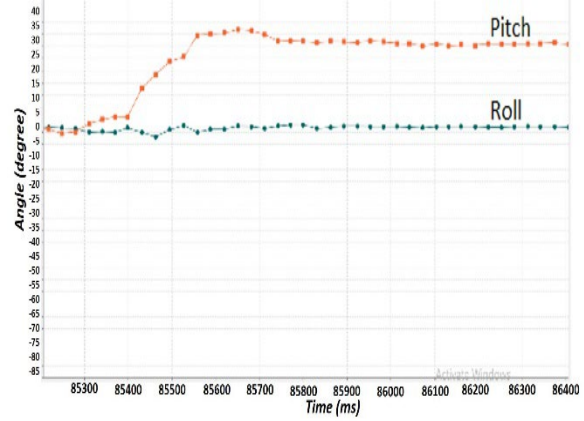


Fig. 13. Orientation angles when changing from standing upright to leaning forward

4.2. Experimental Results for Body States

According to the definition of states given above, together with the experimental results obtained in Table 1, the results for states which are sets of single actions are listed in Table 4.

Table 4. The limiting thresholds of the parameters for the body states

Parameter	Stable state	Fallible state	Failed down state
a_x	(-0.3; 0.3)g	(-0.5; -0.3) v(0.3; 0.5)g	-
a_y	(-0.3; 0.3)g	(-0.5; -0.3) v(0.3; 0.5)g	-
a_z	(-1.0; -0.8)g	(-0.8; -0.75)g	-
A	(0.9; 1.0)g	(0.9; 1.0)g	(1.25; 3)g
α	(-15; 15)°	(-35; -20)° v(20; 35)°	(-90; -60)° v(60; 90)°
β	(-15; 15)°	(-35; -20)° v(20; 35)°	(-90; -60)° v(60; 90)°

4.3. Recognition Results for Body States

The experiment is based on single actions tested with different body states. The body state recognition results are sent to a Bluetooth communication application on a mobile phone as shown in Fig. 14. This application is designed with a simple interface created on the MIT APP INVENTOR platform to collect data of body states.

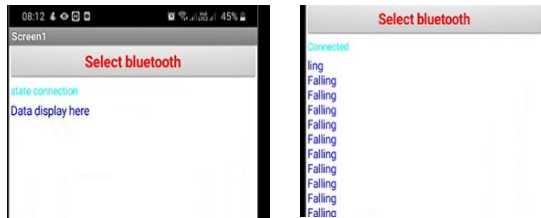


Fig. 14. Data collection Bluetooth app interface

This application is developed to make the wearable device a monitoring device used on caregivers' phones and has a warning function when the elderly falls or slips. The body state recognition experiments were performed in 30 separate times for each state. The results of this experiment are listed in Table 3. From this table, the results of correct detection for stable state, fallible state, and slipped down state are 93.33%, 86.67%, and 96.67%, respectively. The reason why the slipped down state receives highest ratio of recognition is maybe due to quite clear occurrence with the threshold more pronounced than the other two states. Meanwhile, the fallible state achieves lowest accuracy of recognition because this state may be the state in between stable and falling posture which means the body is tilting or tending to approach the stable or slipping down. More trials can be carried out to make the thresholds to reach more

appropriate values and increase the recognition accuracy.

4.4. Heart rate Measurement

Experiments to measure heart rate was performed at 30 different trials. The testing subject is a 22-year-old male with normal health, without cardiovascular disease. The heart rate results at the different sampling times are listed in Table 5.

Table 5. Heart rate measurement result

Trial	1	2	3	4	5	6	7	8	9	10
BPM	97	92	91	90	98	100	95	99	96	104
Trial	11	12	13	14	15	16	17	18	19	20
BPM	88	102	91	93	96	96	98	100	97	98
Trial	21	22	23	24	25	26	27	28	29	30
BPM	94	91	95	95	104	98	97	99	93	90

Since we integrated the ECG sensor with the other motion sensors, the heart rate measurement had some deflection in the heart rate monitor. However, from Table 5, it can be seen that the heart rate measurement results mainly focus on the range of 91 - 97 beats/min. Based on the ideal heart rate for each age mentioned in Table 1, it can be computed that this result is 90% accurate for the test subject because for healthy adults, the 60 to 100 bpm is the suitable value.

5. Conclusion

In this study, a wearable device for fall and slip detection and warning for the elderly people was successfully designed and tested. This device is constructed based on the threshold principle in which the movement sensors were mainly used and implemented. Through the test results obtained above, it can be seen that the detection functions originally set out for the device have basically been implemented. For the body state recognition results, it demonstrates that the recognition results are not really high but acceptable and feasible for a device in the process of testing. The results of the identification of steady state and the slipped state that can slip obtained at 93.33% and 96.67%, respectively, showing that the classification of actions in these states is appropriate. The fact for fallible state shows that in the boundary regions of the parameter thresholds for these two states, there is overlap leading to misidentification. In the future, with the more trial tests, the results can be significantly improved.

Acknowledgments

This research is funded by Hanoi University of Science and Technology (HUST) under project number T2023-TĐ-012.

References

- [1] Sharif, S. I., Al-Harbi, A. B., Al-Shihabi, A. M., Al-Daour, D. S. and Sharif, R. S., Falls in the elderly: assessment of prevalence and risk factors. *Pharmacy Practice (Granada)*, 16(3), 2018.
<https://doi.org/10.18549/PharmPract.2018.03.1206>
- [2] Takashima, K., Wada, K., Tra, T. T. and Smith, D.R., A review of Vietnam's healthcare reform through the Direction of Healthcare Activities (DOHA). *Environmental Health and Preventive Medicine*, 2017, 22(1), pp.1-7.
<https://doi.org/10.1186/s12199-017-0682-z>
- [3] Hoang, D. K., Le, N. M., Vo-Thi, U. P., Nguyen, H.G., Ho-Pham, L. T. and Nguyen, T. V., Mechanography assessment of fall risk in older adults: the Vietnam Osteoporosis Study. *Journal of Cachexia, Sarcopenia and Muscle*, 2021.
<https://doi.org/10.1002/jcsm.12751>
- [4] Mubashir, M., Shao, L. and Seed, L., A survey on fall detection: Principles and approaches, *Neurocomputing*, 100, 2013, pp.144-152.
<https://doi.org/10.1016/j.neucom.2011.09.037>
- [5] Kadhum, A.A., Al-Libawy, H. and Hussein, E.A., May. An accurate fall detection system for the elderly people using smartphone inertial sensors. In *Journal of Physics: Conference Series (Vol. 1530, No. 1, p. 012102)*, 2020.
<https://doi.org/10.1088/1742-6596/1530/1/012102>
- [6] Aguiar, B., Rocha, T., Silva, J. and Sousa, I., June. Accelerometer-based fall detection for smartphones. In *2014 IEEE International Symposium on Medical Measurements and Applications (MeMeA) 2014*, pp. 1-6. IEEE.
<https://doi.org/10.1109/MeMeA.2014.6860110>
- [7] Wang, F.T., Chan, H. L., Hsu, M. H., Lin, C. K., Chao, P. K. and Chang, Y. J., Threshold-based fall detection using a hybrid of tri-axial accelerometer and gyroscope. *Physiological Measurement*, 39 (10), 2018, p.105002.
<https://doi.org/10.1088/1361-6579/aae0eb>
- [8] Lin, C. L., Chiu, W. C., Chu, T. C., Ho, Y. H., Chen, F. H., Hsu, C. C., Hsieh, P. H., Chen, C. H., Lin, C. C. K., Sung, P. S. and Chen, P. T., Innovative head-mounted system based on inertial sensors and magnetometer for detecting falling movements. *Sensors*, 20(20), 2020, p.5774.
<https://doi.org/10.3390/s20205774>
- [9] Trkov, M., Chen, K., Yi, J. and Liu, T., Inertial sensor-based slip detection in human walking. *IEEE Transactions on Automation Science and Engineering*, 16(3), 2019, pp.1399-1411.
<https://doi.org/10.1109/TASE.2018.2884723>
- [10] Mubashir, M., Shao, L. and Seed, L., A survey on fall detection: Principles and approaches. *Neurocomputing*, 100, 2013, pp.144-152
<https://doi.org/10.1016/j.neucom.2011.09.037>
- [11] Sixsmith, A. and Johnson, N., A smart sensor to detect the falls of the elderly. *IEEE Pervasive computing*, 3(2), 2004, pp.42-47.
<https://doi.org/10.1109/MPRV.2004.1316817>
- [12] Jefiza, A., Pramananto, E., Boedinoegroho, H. and Purnomo, M. H., September. Fall detection based on accelerometer and gyroscope using back propagation. In *2017 4th International Conference on Electrical Engineering, Computer Science and Informatics (EECSI)*, 2017, pp. 1-6. IEEE.
<https://doi.org/10.1109/EECSI.2017.8239149>
- [13] Ren, L. and Peng, Y., Research of fall detection and fall prevention technologies: A systematic review. *IEEE Access*, 7, 2019, pp. 77702-77722.
<https://doi.org/10.1109/ACCESS.2019.2922708>
- [14] Harari, Y., Shawen, N., Mummidisetty, C. K. *et al.* A smartphone-based online system for fall detection with alert notifications and contextual information of real-life falls. *J NeuroEngineering Rehabil* 18, 124, 2021.
<https://doi.org/10.1186/s12984-021-00918-z>
- [15] Wayan Wiprayoga Wisesa, I., & Mahardika, G., Fall detection algorithm based on accelerometer and gyroscope sensor data using Recurrent Neural Networks. *IOP Conference Series: Earth and Environmental Science*, 258, 012035, 2019.
<https://doi.org/10.1088/1755-1315/258/1/012035>
- [16] Y. Shao, X. Wang, W. Song, S. Ilyas, H. Guo, and W. S. Chang, Feasibility of Using Floor Vibration to Detect Human Falls, *International Journal of Environmental Research and Public Health*, vol. 18, no. 1, p. 200, Dec. 2020
<https://doi.org/10.3390/ijerph18010200>